

Numerical Study of Relationship Between Landslide Geometry and Run-out Distance of Landslide Mass

Muneyoshi Numada

Research Associate, Institute of Industrial Science, The University of Tokyo, Japan

Kazuo Konagai

Professor, Institute of Industrial Science, The University of Tokyo, Japan



SUMMARY

The parameters that control the run-out distance of landslides mass are geometry, physical property and frictional coefficients to observe the contribution to run-out distance. For different lengths of the landslide mass, the mass movement is examined in the time-marching calculation of MPM. Lengths of the landslide mass segments L_1 and L_2 on the flat and inclined sliding surfaces are obtained respectively at every time step. Also analysis of the effect of width of a landslide mass is carried out. As the width increases, the curve converges on the plane-strain solution. The ultimate load capacity would be more crucial in determining its distal reach. This research introduced some results for extracting important pieces of information for landslide risk assessment from numerical model and real landslide masses. For coherent mass movements, numerical simulation of landslide mass movements using MPM did hint an idea for extracting parameters from real landslide masses. This knowledge will provide a good perspective for landslide risk assessments.

Keywords: Material Point Method, landslide, run-out distance

1. INTRODUCTION

Landslide dangerous area, where are a debris flow, a steep slope collapse and slope failure and so on exist, are found more than 200,000 places in the whole Japan. Landslides can range in size from small movements of loose debris to massive collapses of entire summits. For short to medium-length slopes, installing preventive drainage works, anchoring and/or reinforcing slopes will be effective for assessing and mitigating landslide hazards. However for extremely large slope failures, it is very difficult to mitigate and thus the importance of run out analysis emerges. Many landslides with limited internal deformation will move as coherent masses on thin mobile basal layers. However, others will become flow-like in character after running some long distances, though exhibiting some solid features at their early stages of failure. It is important to forecast the run out distance of landslides mass to reduce the landslide disaster.

This research aims to analyse the key parameter that control the run-out distance of landslides mass. The numerical analysis is an effective approach to analyse the dynamic mechanism of the landslide. For numerical analysis, Material Point Method (MPM) is used in this research.

2. LANDSLIDE PARAMETERS AND MODELING

2.1. Landslide parameters

The type of landslide can be described by the point of various different kinds of sliding mass material and the movement mode. According to the USGS publication, a classification system based on these parameters is shown in Fig. 2.1. In addition to that, other parameters such as form of landslide mass and coefficient of friction are also important to deal with landslide movement. The form of landslide is one of the important measurable parameter and can describe its scale and size. The movement of

landslide mass can be different from its initial form or scale. In this research, the relationships between the different forms such as initial length, width of landslide mass and landslide movement are examined.

2.2. Modelling of landslide mass

The MPM is categorized as one of the mesh-less methods formulated in an arbitrary Lagrangian-Eulerian description of motion (Sulky 1994). In MPM, a body is to be analysed as a cluster of material points. Material Point has information of physical properties on a peculiar position and the stress, etc. The material points, which carry all Lagrangian parameters, can move freely across cell boundaries of a stationary Eulerian lattice, and the information is distributed to each node of belonging cells. This mesh is called as computational mesh, should cover the virtual position of the analysed body. The computational mesh can remain constant for the entire computation, thus the main disadvantage of the conventional finite element method related to the problem of mesh distortions is eliminated for large deformation of soils (Fig. 2.2).

All Lagrangian parameters for the entire landslide mass are hardly obtained. For example, it is often that the plants growing on a landslide mass shoot their roots all through the soil mass. In such a way that overall characteristics of the soil mass is largely different from those obtained through test of soil samples taken point-wise from the landslide mass.

The condition requested for the numerical analysis includes two following elements: 1. Large deformation of soil; and 2. Input parameters composed of information which can be measured. Input parameters applied in MPM model are slope form (geographical features and slide surface), physical properties of deformation of sliding mass (geological features) and physical properties of sliding surface.

A lot of parameters that constitute physical properties of landslide are taken into real landslide phenomenon, but the pseudo-three dimensional model can reduce the number of complex parameters as much as possible (Hungr 1995). The landslide mass is considered to be equivalent fluid in this model and modelling it as assemble of soil columns. In such a model, complex landslide model can be expressed by the interactive force between soil columns, basal force and reducing necessary parameters. Therefore, there is an advantage that the computational complexity can be decreased at the computing lead time (Konagai 2002, Numada 2003 and Abe 2004).

LANDSLIDE CAUSES (USGS)
1. Geological causes
a. Weak or sensitive materials
b. Weathered materials
c. Sheared, jointed, or fissured materials
d. Adversely oriented discontinuity (bedding, schistosity, fault, unconformity, contact, and so forth)
e. Contrast in permeability and/or stiffness of materials
2. Morphological causes
a. Tectonic or volcanic uplift
b. Glacial rebound
c. Fluvial, wave, or glacial erosion of slope toe or lateral margins
d. Subterranean erosion (solution, piping)
e. Deposition loading slope or its crest
f. Vegetation removal (by fire, drought)
g. Thawing
h. Freeze-and-thaw weathering
i. Shrink-and-swell weathering
3. Human causes
a. Excavation of slope or its toe
b. Loading of slope or its crest
c. Drawdown (of reservoirs)
d. Deforestation
e. Irrigation
f. Mining
g. Artificial vibration
h. Water leakage from utilities

Figure 2.1. Landslide parameters (USGS)

3. NUMERICAL SIMULATION

3.1. Length of landslide mass and run-out distance

For landslide mass is modeled in MPM, width of the landslide W and depth H are made constant, the landslide length is set different six pattern from 20 to 100m length (Fig. 3.1). The initial thickness H of the landslide mass is set to 1m. A rectangular-planner soil mass of 1m thick is assumed to be resting on a flat slope dipping to a level ground, which spreads in immediately front of the toe of the landslide mass.

The slope angle of MPM model is set uniformly to 20 degrees. The coefficient of friction is set separately on the slope side and flat surface side, and the coefficient of flat surface side μ_1 and slope side μ_2 are 0.8 and 0.2 respectively (Table 3.1).

The Young's modulus of the landslide mass E is taken as 2×10^6 Pa, poisson's ratio is 0.3, internal frictional angle ϕ is set to 30 degrees, cohesion C is derived from Rankin's earth pressure model to stand upright 1m height in the gravity. Drucker-Prager model is used as the constitutive law of landslide mass in this research. The initial material point for one cell arranges to be 2×2 for $0.2\text{m} \times 0.2\text{m}$ size cell.

For different lengths of the landslide mass L , the mass movement is examined in the time-marching calculation of MPM (Fig. 3.2). The run-out distance L_1 is defined as the distance from boundary of slope-flat surface zone to head of the landslide mass, and L_2 is the distance of the landslide mass that remains of a slope side. These are obtained at every time step. The average stress σ_a is the average value of the stress that acts upon the boundary on a slope and flat side. The average stress σ_a is calculated the average value of the stress of node on the boundary between a slope and a flat surface side. Initially landslide mass keeps $L_1 + L_2$ to be completely identical to the entire length of the landslide mass L . To be exact, the entire length is kept unchanged (Fig. 3.3).

However, as the landslide mass runs further forward over the level ground (deposition zone), its movement slows down due to larger frictional coefficient and with no driving force induced on the level ground. Eventually the following segment of the landslide mass pushes the soil from behind, and immediately after the ultimate load capacity F , the average stress σ_a reaches peak strength σ_p , that the limit landslide mass can sustain is reached and $L_1 + L_2$ value starts shrinking ($L_1 + L_2 < L$). For long landslide masses, L_1 converges on a constant value, ultimate L_{1y} , suggesting that the entire length of the landslide mass has little or nothing to do with the ultimate load capacity (Fig. 3.4). In the other word, there is the upper bound of distal reach of the landslide mass. It will be also a matter of course that L_2 can converge likewise on a particular value, ultimate L_{2y} , with the presence of the ultimate load F .

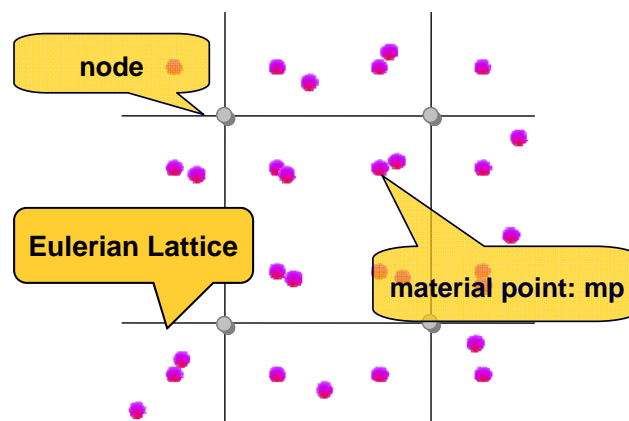


Figure 2.2. Eulerian lattice and material points

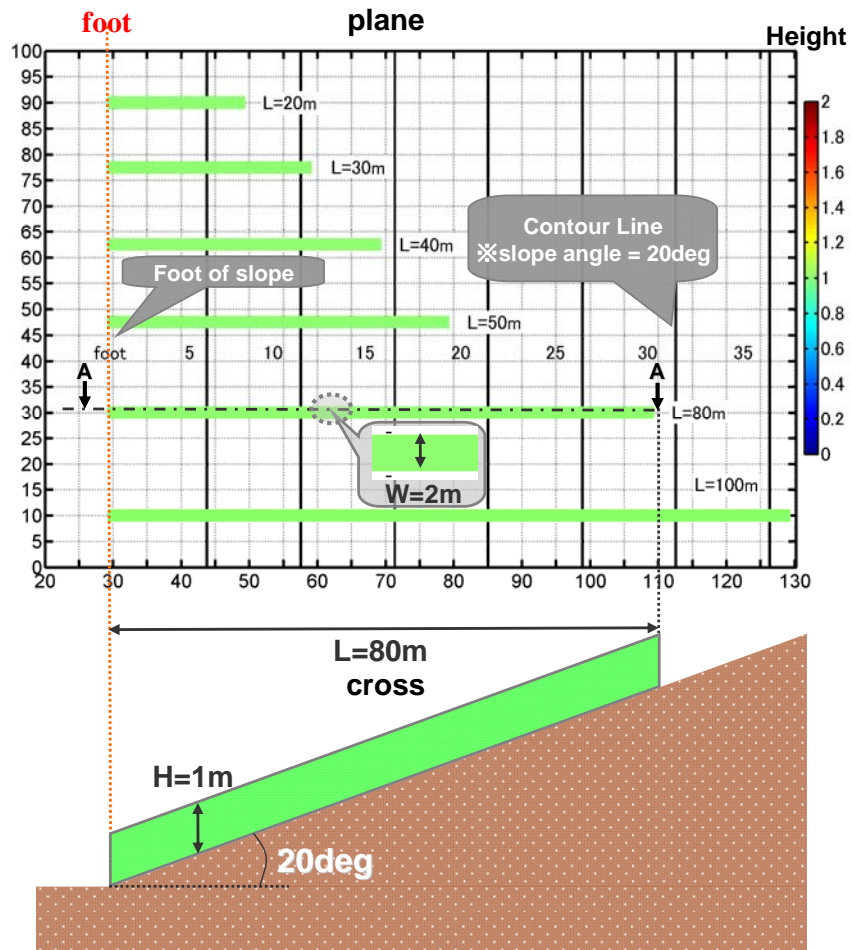


Figure 3.1. MPM model for different length of landslide mass (upper: plane view, lower: cross)

Table 3.1. Parameters of landslide mass and MPM setting

Parameter	Value
Sliding surface dip	20 deg
μ_1 (flat surface)	0.8
μ_2 (slope surface)	0.2
ϕ (soil mass)	30 deg
Young's modulus	2×10^6 Pa
Poisson's ratio	0.3
Density	1600 kg/m^3
Cell size	$0.2\text{m} \times 0.2\text{m}$
Initial arrangement of particles in a cell	2×2
Time increment	5×10^{-4}

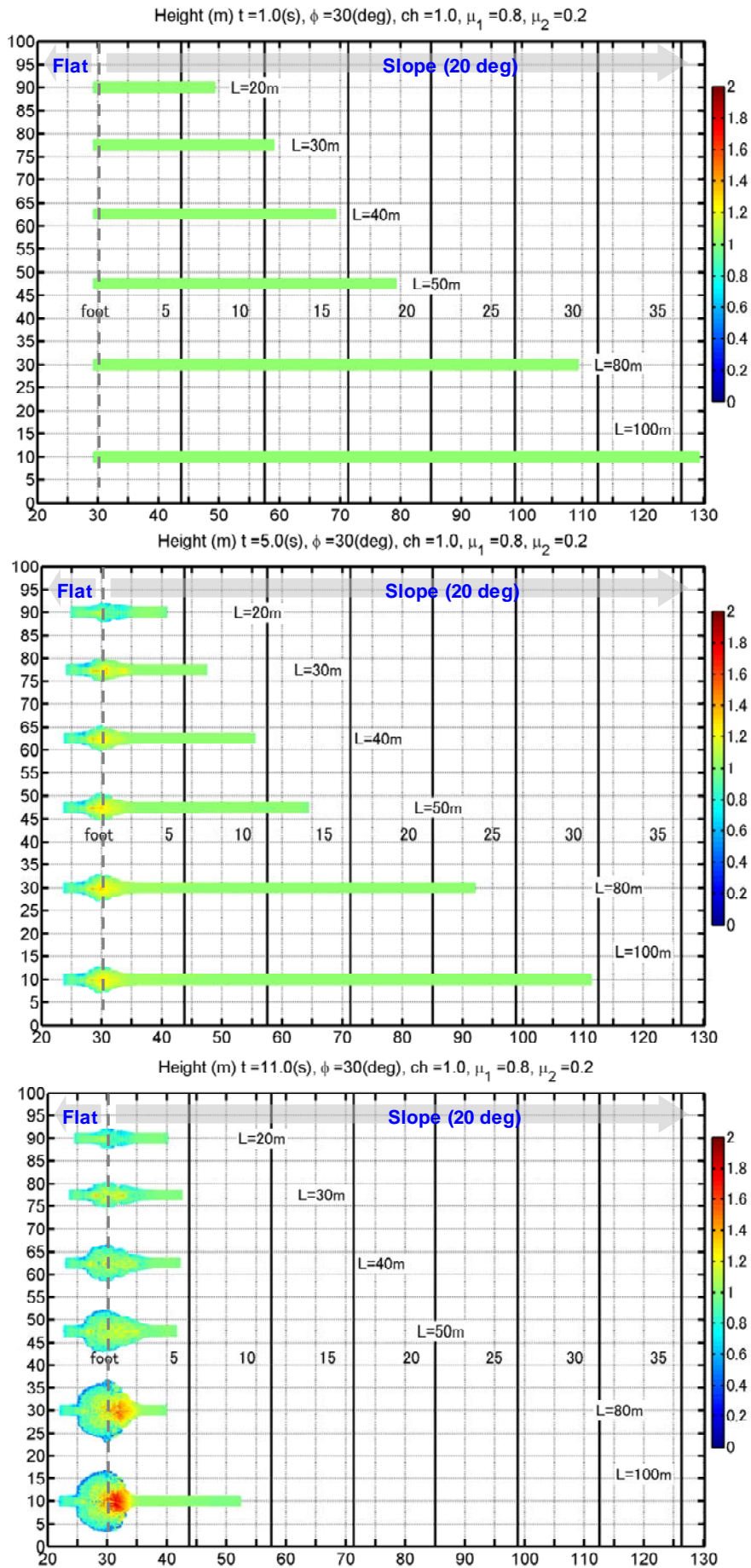


Figure 3.2. Plane view of numerical result for different length of landslide mass (time 1s-15s)

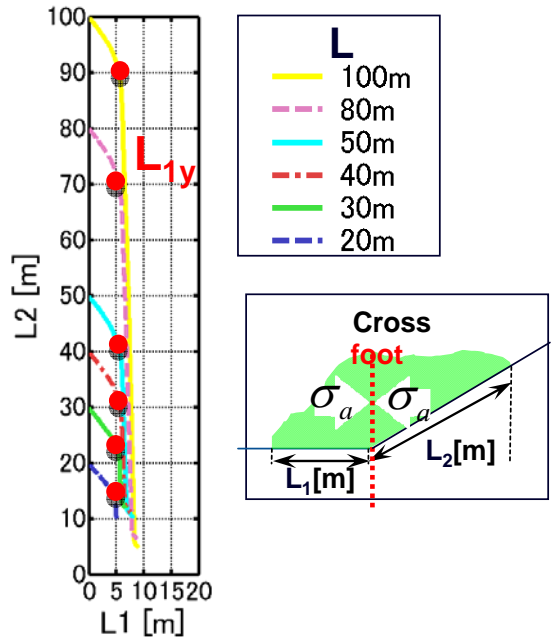


Figure 3.3. Relationship between L_1 and L_2 for different length of landslide mass

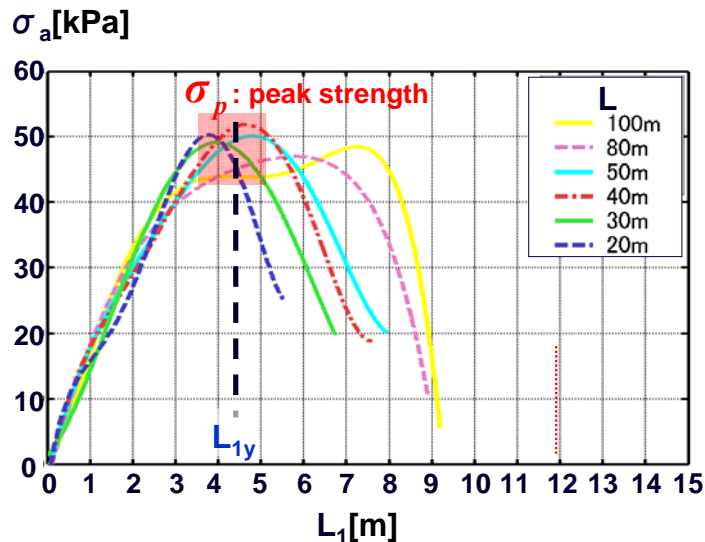


Figure 3.4. Relationship between L_1 and the average stress σ_a for different length of landslide mass

3.2. Width of landslide mass and run-out distance

Width of a landslide mass can also affect F and therefore L_{1y} and L_{2y} , as the width increases, the curve converges on the plane-stress solution for thinner soil cases (Fig. 3.5). In Fig. 3.6, after the landslide mass starts yielding, dL_2/dL_1 becomes less steep for wider soil masses. This can be explained as follows: This dL_2/dL_1 , when multiplied by the cross-sectional area of the landslide mass, is identical to $-dV_2/dV_1$, where dV_2 and dV_1 are soil volumes which pass through the cross section per unit time for segments L_1 and L_2 , respectively.

The soil volume dV_1 will be pushed forward over the deposition zone by the following soil volume dV_1 , while the volume of $dV_2 - dV_1$ is pushed up and/or sideways making a bulge at around the toe of the slope. It is clear that, less steep dV_2/dV_1 indicates larger confinement of $dV_2 - dV_1$ causing slight increase of the average stress σ_a even after the initial ultimate capacity σ_p was reached (Fig. 3.7). In other words, the effect of confinement can be quantitatively estimated from geometry of the deformed landslide mass.

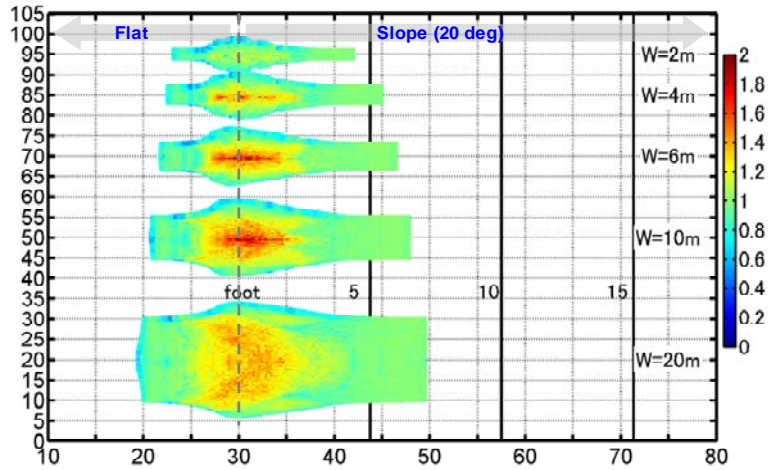


Figure 3.5. Plane view of numerical result for different width of landslide mass (time 10s)

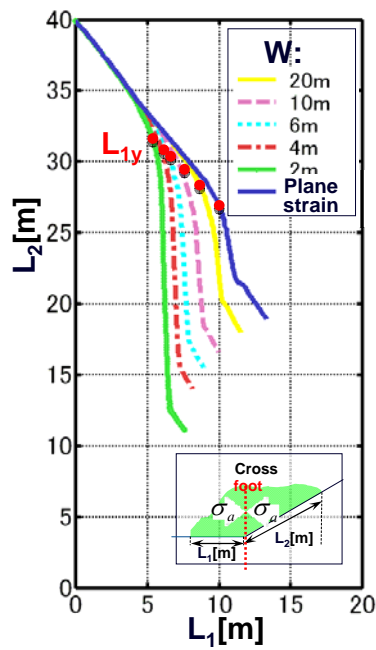


Figure 3.6. Relationship between L_1 and L_2 for different width of landslide mass

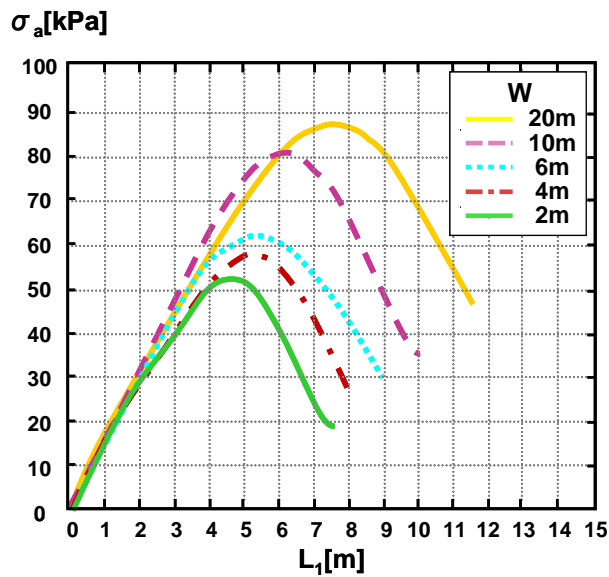


Figure 3.7. Relationship between L_1 and the average stress σ_a for different width of landslide mass

Width of a landslide mass can also affect F . As the width increases, the curve converges on the plane-strain solution, while it is rather closer to plane-stress solution for thinner soil cases. The ultimate load capacity F would be more crucial in determining its distal reach. In this research, by analysis on different width of the landslide, as the confining pressure is increasing, peak stress is increasing; it becomes a phenomenon similar to tri-axial compression tests.

4. CONCLUSION

This research introduced some results for extracting important pieces of information for landslide risk assessment from numerical model and real landslide masses. For coherent mass movements, numerical simulation of landslide mass movements using Material Point Method (MPM) gave an idea for extracting parameters from real land slide masses. A real cohesive landslide can be viewed as a large-scale specimen of a monotonic loading test for obtaining its ultimate load capacity, which can be greatly responsible for distal reach of the landslide mass. And also, the coefficient of sliding surface that is one of the important parameter to define run-out distance on the deposit zone is difficult to be evaluated from real site. For that one possible approach is proposed in this research. This knowledge will provide a good perspective for landslide risk assessments.

REFERENCES

- Abe, K., Numada, M. and Konagai, K. (2004). A method and its problems for numerical analysis of rapid and long traveling soil flows, *Seisan kenkyu, The University of Tokyo, IIS*, **56: 6**, pp. 487-491.
- Hung, O. (1995). A model for the run out analysis of rapid flow slides, debris flows, and avalanches, *Canadian Geotechnical Journal*, **32**, pp. 610-623.
- Konagai, K. and Numada, M. (2002). Pseudo-three dimensional lagrangian particle finite difference method for modeling long-traveling soil flows, *Journal of Dam engineering*, **12:2**, pp. 123-128.
- Numada, M., Konagai, K., Ito, H. and Johansson, J. (2003). Material point method for run out analysis of earthquake-induced long-traveling soil flows, *Journal of Earthquake Engineering*, **27**, Paper-number 0276.
- Sulky, D., Chen, Z. and Schreyer, H.L. (1994). A particle method for history dependent materials. *Computer methods in applied mechanics and engineering*, **118**, pp. 179-196.
- U.S. Geological Survey: Landslide Types and Processes, <http://pubs.usgs.gov/fs/2004/3072/pdf/fs2004-3072.pdf>